17 Oct 2018

Influence Of Higher-order Modes In Coaxial Waveguide On Measurements Of Material Parameters

Dmitry A. Petrov

Konstantin N. Rozanov
Missouri University of Science and Technology, rozanovk@mst.edu

Marina Y. Koledintseva
Missouri University of Science and Technology, marinak@mst.edu

Recommended Citation

D. A. Petrov et al., "Influence Of Higher-order Modes In Coaxial Waveguide On Measurements Of Material Parameters," *2018 IEEE Symposium on Electromagnetic Compatibility, Signal Integrity and Power Integrity, EMC, SI and PI 2018*, article no. 8495305, Institute of Electrical and Electronics Engineers, Oct 2018.
The definitive version is available at https://doi.org/10.1109/EMCSI.2018.8495305

Influence of Higher-order Modes in Coaxial Waveguide on Measurements of Material Parameters

Dmitry A. Petrov[#1], Konstantin N. Rozanov [#2] and Marina Y. Koledintseva [*3]

[#] *Institute for Theoretical and Applied Electromagnetics, 13 Izhorskaya ul., 125412 Moscow, Russia, *Oracle, 4090 Network Cir., Santa Clara, CA 95054, USA*

[1] dpetrov-itae@yandex.ru, [2] k_rozanov@mail.ru, [3] marina.koledintseva@oracle.com

Abstract— **The use of a coaxial air-filled line as a test fixture for measuring complex permittivity and permeability often shows odd resonance-like behavior of material parameters as functions of frequency. This effect is typically either ascribed to the half-wavelength resonance at the sample length, or erroneously misinterpreted as intrinsic resonance behavior of the material. However, as is shown in this paper, such behavior can be attributed to excitation of the higher-order modes on the surface of the sample resulting in resonance absorption of electromagnetic energy in the test fixture. Herein, analytical, numerical, and experimental results show that there can actually be a significant impact of higher-order modes in a coaxial line on the extracted constitutive material parameters of samples.**

I. Introduction

Accurate wideband measurements of the permittivity and permeability of materials are always of demand, especially as new advanced materials for various electromagnetic applications are engineered [1].

The Nicolson-Ross-Weir (NRW) technique allows for measuring the frequency-dependent complex permittivity $\varepsilon = \varepsilon' - j\varepsilon''$ and permeability $\mu = \mu' - j\mu''$ in the microwave range [2], [3]. The method is based on measuring complex reflection and transmission coefficients from a sample fully filling the cross-section of a waveguide of air-filled coaxial line test fixture. Using a vector network analyzer (VNA) or a time-domain reflectometer (TDR), S-parameters of the two-port test fixture with a sample are measured, and complex ε and μ are extracted simultaneously.

Coaxial air-filled transmission lines are currently the most popular test fixtures for wideband measurements of dielectric and magnetic properties of material samples of any loss, from low to high.

The requirement for using the NRW technique is to prepare a proper test sample. For an air-filled coaxial line, test samples should have washer shape of certain thickness. To avoid measurement errors, the sample should have smooth parallel planes normal to the axis of the test fixture, and its inner and outer diameters should fit properly the dimensions of the line cross-section with minimum possible gaps and voids. The sample thickness should be such that the resonance between its parallel planes falls beyond the highest operation frequency of the test fixture, *i.e.*, for the materials with high permittivity and/or permeability, thin samples are used. The sample thickness should satisfy the inequality

$$d < \frac{\lambda_{0\min}}{2\sqrt{\varepsilon'_r \mu'_r}}, \quad (1)$$

where $\lambda_{0\min}=c_0/f_{\max}$ is the minimum wavelength of TEM in air corresponding to the maximum operational frequency of the coaxial air-filled test line, and ε'_r and μ'_r are the real parts of relative permittivity and permeability of the sample, respectively. To assure that inequality (1) is satisfied when running measurements, it is recommended to estimate the highest expected values of constitutive parameters over the frequency range of interest. In majority of cases, these are the static or low-frequency values of permittivity and permeability.

However, even if (1) is satisfied, measurements of ε and μ of a test sample may result in an odd resonance-like behavior, which is not due to either half-wavelength resonance on the material sample length, or the calibration error, or any intrinsic resonances of material constitutive parameters. An example of such behavior is shown in Fig. 1; the data was obtained from the measurements of a washer-shaped sample made of a composite material placed in the standard coaxial air-filled test fixture. The composite was made of wax filled with non-magnetic conductive powder particles. It is seen that the frequency dependences of material parameters are significantly distorted. The distortion may become especially problematic when measuring thicker samples in a wide frequency range.

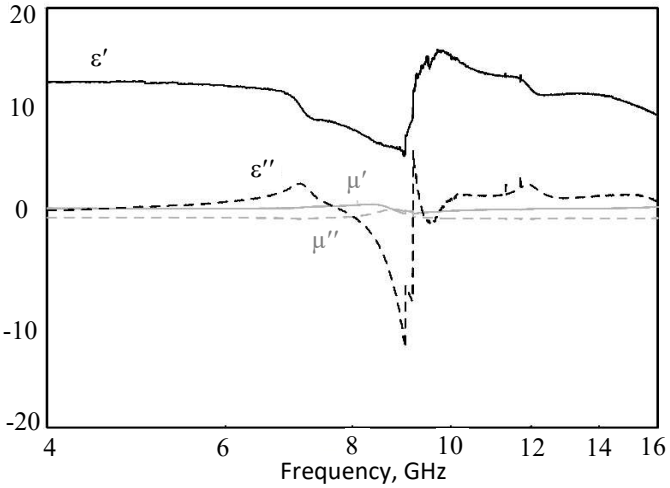

Fig. 1. The measured frequency dependence of complex permittivity (black) and permeability (gray) of a composite sample with multiple resonances, with proper calibration and port effects removal

Such resonance behavior as in Fig. 1 can be easily misinterpreted as an actual property of the material under study. However, at microwave frequencies, usually only permeability

may demonstrate resonance behavior, which typically occurs due to spin resonance, domain walls motion, or skin effect [4]. As for permittivity of solid materials, resonance absorption in microwave band is comparatively rare. Moreover, it is practically impossible that magnetic and dielectric resonances in a material would take place at the same frequency. Therefore, resonance behavior of frequency dependence of the permittivity should always be examined with scrutiny before any major conclusions are made.

In this paper, we suppose that the cause of the parasitic resonance behavior observed in the measurements, as in Fig.1, may be the higher-order modes in samples inside a waveguiding structure. Note that the emerging and propagating higher order modes at the materials characterization in transmission lines is of great interest [5], [6].

Therefore, the objective is to show that the higher-order mode resonances excited in a washer-shaped sample along its circumference are actually responsible for additional resonances seen on measured frequency dependences of material parameters. The resonance effect of the higher-order modes on the measured permittivity in a standard air-filled coaxial line is studied experimentally and verified using analytical computations and numerical electromagnetic modeling. The measurements are conducted over the frequency range from 100 MHz to 20 GHz on non-magnetic composite samples. The way to minimize this effect is proposed, and it is mainly related to the quality of the sample preparation and the proper thickness.

II. Experiment

The composite material for test samples was made by mixing copper particles with molten wax and cooling down at constant stirring to reduce the effect of particle agglomerations.

The experiments with samples were conducted using Agilent 8720C VNA and Rosenberger N-Type beadless 7/3-mm air-filled coaxial line 26.4 mm long used as a sample holder. Four toroid (washer-shaped) samples were made with inner and outer diameters of 3 mm and 7 mm, respectively, so that the samples would completely fill the cross-section of the coaxial waveguide. The samples thicknesses varied from 1.47 mm to 5.23 mm and were measured with ±0.03 mm accuracy using a precision caliper.

Permittivity and permeability of the composite material were calculated using the NRW method from the measured S-parameters of the test fixture with each sample inside it. The samples of various thicknesses were studied in order to observe the resonance frequency variation. The samples were formed from a single chunk of a non-magnetic composite material and thus had identical density and intrinsic microstructure. The extracted relative permittivity of all the samples was the same, ε_r=13-j0.3 (see the low-frequency region in Fig. 1).

The power loss in the coaxial line with each of the four test samples was measured over the frequency range from 100 MHz to 20 GHz. The characteristics are shown in Fig. 2 starting at 5 GHz, since at the lower frequencies the curves are monotonic. The distinct energy loss pattern that corresponds to the half-wavelength interference effect with additional resonance absorption is shown in this figure. Arrows show the frequencies of the lowest higher-mode resonance excited in these samples. The thinner samples, d=1.47 mm and d=2.83 mm, exhibit the more pronounced resonances at frequencies of 10.3 GHz and 8.59 GHz, respectively. The resonance frequencies observed in the thicker samples, d=4.1 mm and d=5.23 mm, have the lower quality factors Q and are located at 7.52 GHz and 7.24 GHz, respectively.

The higher-order modes may also contribute to calibration and measurement errors due to mismatches at the connectors when changing the coaxial calibration standards, as seen in Fig. 2 in the region of sharp resonances around 18-19 GHz.

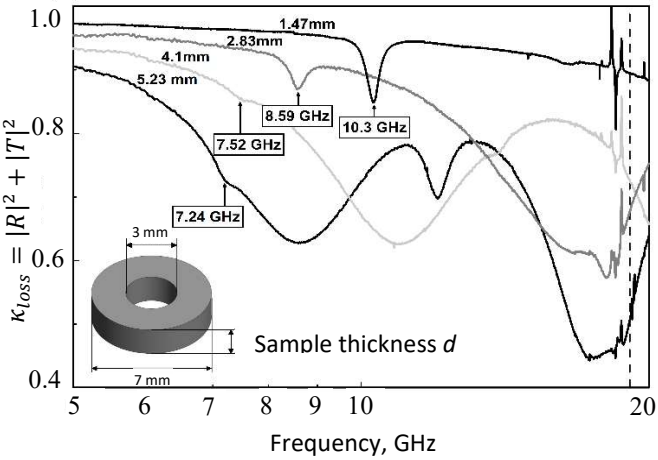

Fig. 2. A sample view and frequency dependences of power loss in test samples of various thicknesses. Arrows show the lowest higher mode resonance for each sample thickness. Dashed vertical line shows the upper frequency for standard 7/3-mm coaxial lines single TEM mode operation.

III. Numerical Simulations

The 3D full-wave numerical electromagnetic experiments were conducted using a commercial software FEKO [7]. The numerical model setup includes a coaxial line structure, a sample with material parameters close to those in the physical experiment, and waveguide ports with a single TEM mode excited. The numerical model setup is shown in Fig. 3 (a). The model segments are indicated in Fig. 3 (b). Although the higher modes can propagate in the sample, they have to emerge in the first place on the boundary of the sample. In the ideal case, when the sample is perfectly homogeneous and sample surfaces are strictly perpendicular to the Poynting vector, the resonance absorption due to higher modes will not manifest itself. To demonstrate qualitatively the higher modes generation in the numerical experiment, one of the surfaces of the samples was slightly tilted as is shown in Fig. 3.

Note that the correlation between the imperfect (inhomogeneous, with voids, etc.) sample under test and excitation of higher-order modes by conversion from TEM mode to higher-order mode was pointed out in [8].

The modeled transmission coefficient magnitudes for a coaxial line containing a composite material sample, with sample thickness varying from 0.2 cm to 0.6 cm, are shown in Fig. 4. The line length was the same as in experiments, 26.4 mm. The complex permittivity of the samples in the models is taken as ε_r=13–j0.3 (see the low-frequency values for

permittivity in Fig. 1), and permeability is μ_r=1. Wave ports with a single TEM mode were excited. Resonances on each of the modeled curves are indicated in Fig. 4.

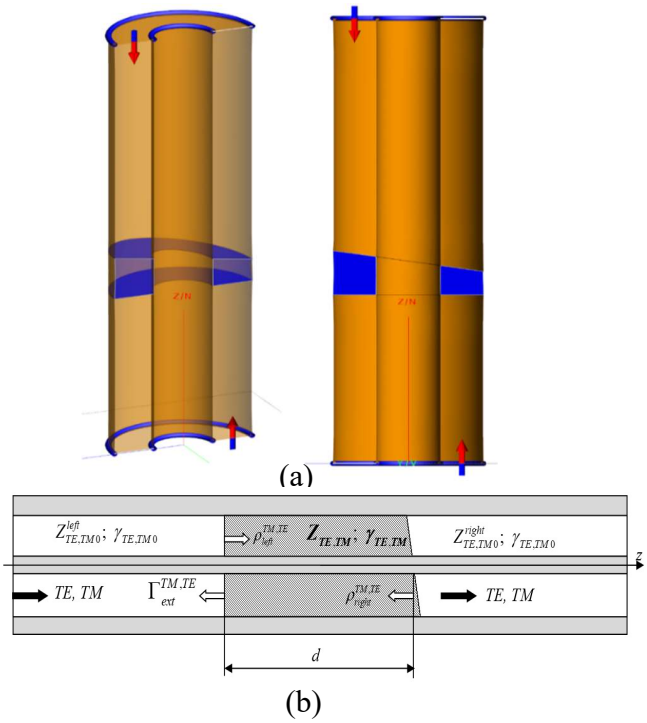

Fig. 3. Coaxial waveguide structure with a sample, FEKO model (a) and reflections (b) at the boundaries between air and sample in a coaxial test fixture.

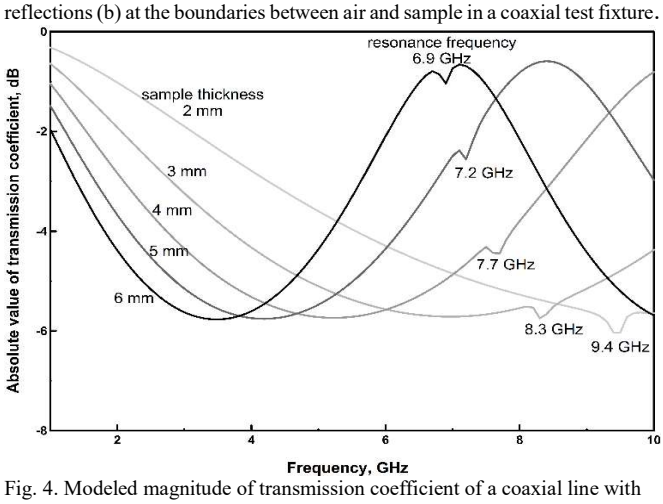

Fig. 4. Modeled magnitude of transmission coefficient of a coaxial line with samples with skewed surface of composite material of different thicknesses

Comparing Figs. 2 and 4, one can see that the resonance dips at 7.52 GHz in experiment and 7.69 GHz in the numerical model are close to each other. Since the thickness of the sample is uneven, the average measured thickness is indicated. In the measurements, it is d=4.1 mm. The closest modeled average thickness is d=4 mm. Note that in the numerical experiment, for convenience and clear distinction from the real physical experiment, the sizes where taken with equal step (1 mm). The actual manufactured samples did not have exactly the same thicknesses as numerical data points, because it is not easy to control thickness of samples at their manufacturing process.

Theoretical analysis is needed to understand this resonance behavior, and the objective is to obtain comparable curves from physical and numerical experiments and analytical consideration.

IV. Analytical Formulation

In a coaxial structure with the internal radius r_i and the external radius r_0, in addition to TEM mode, two types of modes may be present – TM and TE. The characteristic impedances of the modes are [9]

$$Z_{TM} = \frac{E_r}{H_\varphi} = \frac{\gamma_{TM}}{\omega\varepsilon} \text{ and } Z_{TE} = \frac{E_r}{H_\varphi} = \frac{\omega\mu}{\gamma_{TE}}, \quad (2)$$

where γ_{TM} and γ_{TE} are calculated from the general expression for the propagation constants for the modes, with the corresponding cut-off angular frequencies ω_c :

$$\gamma = \pm j\sqrt{\omega^2\varepsilon\mu - k_c^2} = \pm j\omega\sqrt{\varepsilon\mu}\sqrt{1-\omega_c^2/\omega^2}\,. \quad (3)$$

The mode TE_{11} in a coaxial line has the lowest cut-off frequency of all the higher-order modes. The electromagnetic field distributions for the fundamental TEM mode and the mode TE_{11} are shown in Fig. 5.

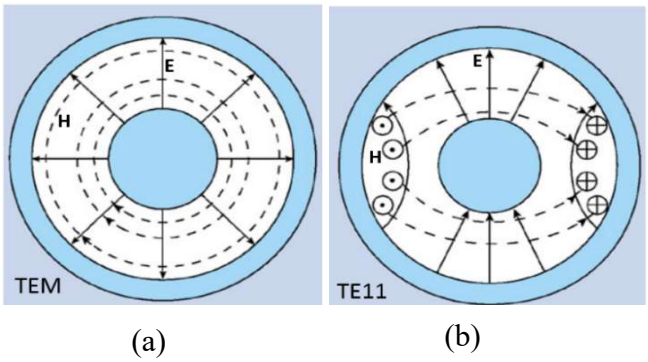

Fig. 5. Electromagnetic field distributions for TEM mode (a) and TE_{11} mode (b) is a coaxial waveguide. Solid lines – E-field, dashed lines – H-field.

The cutoff frequencies for the modes are found as the solutions of the transcendental equations [10]:

$$\frac{N_n(k_c r_i)}{J_n(k_c r_i)} = \frac{N_n(k_c r_0)}{J_n(k_c r_0)} \text{ for TM modes} \quad (4)$$

and

$$\frac{N_n'(k_c r_i)}{J_n'(k_c r_i)} = \frac{N_n'(k_c r_0)}{J_n'(k_c r_0)} \text{ for TE modes,} \quad (5)$$

where J_n are Bessel functions of the 1st kind and N_n are Neumann functions (or Bessel functions of the 2nd kind), and prime signs denote the corresponding derivatives.

For example, for the lowest TE_{11} mode in a coaxial waveguide filled with material having ε_r=13 and cut-off wave number k_c=403.37 m^{-1}, the cut-off frequency is f_c=5.30 GHz and cut-off wavelength λ_c=15.6 mm.

Let us consider the reflections at the flat boundaries of a washer-shaped sample placed in the coaxial line and fully occupying its cross-section. Assume that the line axis z is horizontal, and the electromagnetic wave is incident from the left to the right, as is shown in Fig. 3 (b).

The complex *internal* reflection coefficient at the "sample-air" boundary *inside* the coaxial line on the right-hand side is

$$\rho_{right}^{TM,TE} = \frac{Z_0^{right} - Z_{TM,TE}}{Z_0^{right} + Z_{TM,TE}}; \quad (6)$$

The *internal* reflection coefficient between the sample and the air-filled part on the left-hand side of the coaxial line is

$$\rho_{left}^{TM,TE} = \frac{Z_0^{left} - Z_{TM,TE}}{Z_0^{left} + Z_{TM,TE}}. \quad (7)$$

Note that Z_0^{right} and Z_0^{left} can be different in the general case, but in the symmetrical case (right and left ports are identical), they are equal, $Z_0^{left} = Z_0^{right} = Z_{TE,TM0}$. Each of these depends on the mode type (TE or TM) in the empty coaxial line. Their characteristic impedances are as in (2), but with ε_0 and μ_0 instead of ε and μ.

Applying the transmission line theory concept of the input impedance [9] to TE and TM modes, one can re-calculate the "load" impedance (sample-air) from the right-hand side cross-section to the left-hand side boundary (air-sample) of the sample as

$$Z_{in}^{TM,TE} = Z_{TM,TE} \frac{Z_{TM,TE0} + Z_{TM,TE} \tanh\left(\gamma_{TM,TE} d\right)}{Z_{TM,TE} + Z_{TM,TE0} \tanh\left(\gamma_{TM,TE} d\right)}, \quad (8)$$

where d is the average sample thickness. Then the *external* reflection coefficient at the left-hand side boundary (air-sample), which will correspond to the portion of the S_{11} parameter measured using the VNA due to the contribution of the corresponding higher-order mode is

$$\Gamma_{ext}^{TM,TE} = \frac{Z_{in}^{TM,TE} - Z_{TM,TE0}}{Z_{in}^{TM,TE} + Z_{TM,TE0}}. \quad (9)$$

The same external reflection coefficient can be represented through the internal reflection coefficients (6) and (7) as

$$\Gamma_{ext}^{TM,TE} = \frac{\rho_{left}^{TM,TE} + \rho_{right}^{TM,TE} \exp(2\gamma_{TE,TM} d)}{1 + \rho_{left}^{TM,TE} \rho_{right}^{TM,TE} \exp(2\gamma_{TE,TM} d)}. \quad (10)$$

Due to the symmetry $\rho_{left}^{TM,TE} = \rho_{right}^{TM,TE} = \rho^{TM,TE}$, temporarily omitting *TM,TE* notations and representing each internal reflection coefficient as $\rho = |\rho| e^{j\varphi}$, the following expression can be obtained for the external reflection coefficient in the lossless case ($\gamma_{TE,TM} = \alpha + j\beta$, $\alpha = 0$):

$$|\Gamma_{ext}| = \frac{|\rho| \sqrt{2(1 + \cos(2\beta d))}}{\sqrt{1 + 2|\rho|^2 \cos^2(2\beta d + 2\varphi) + |\rho|^4}}. \quad (11)$$

In the lossy case ($\alpha \neq 0$), the expression analogous to (11) can be obtained through the hyperbolic functions.

The maximum magnitude of the reflection coefficient (11) is achieved at the standing wave node, when the cosine function turns to zero. Therefore, the resonance condition within the sample of the thickness d is

$$2(\varphi + \beta d) = 2\pi n, \quad (12)$$

where n is integer; and φ is the phase of the reflection coefficient as defined above. Physically, this resonance condition means that the total phase progression is the doubled sum of the mode progression along the sample thickness βd and the phase of the reflection coefficient from the sample-air boundary inside the coaxial line at each individual mode. Herein, we are interested in the lowest resonance with n=0.

In the more general form, with the notations for the TM and TE modes, and expanding the propagation constant β based on (3), the resonance condition (12) can be represented as

$$Arg(\rho_{right}^{TE,TM}) + Arg(\rho_{left}^{TE,TM}) + 2\,\mathrm{Im}\left(\frac{2\pi d}{\lambda} \sqrt{\varepsilon_r \mu_r - \left(\frac{f_c}{f}\right)^2}\right) = 0. \quad (13)$$

The proposed model allows for calculating the dependence of the resonance frequency versus sample thickness for the TE_{11} mode in the cases of dielectric samples with ε_r=13–j0.3, as is shown in Fig. 6. It is readily obtained that the cut-off frequency for TE_{11} mode in a coaxial line filled with material with ε_r = 13 is 5.3 GHz (lossless case). The dependence of resonance frequency vs. sample thickness is calculated using (13). The results of the numerical simulations for the sample lengths $d \leq 6$ mm, as well as experimental data points, are also plotted in Fig. 6. As is seen, the agreement between analytical, numerical, and experimental data is good. Maximum discrepancy is below 5% for all the data points, slightly increasing as the sample thickness increases.

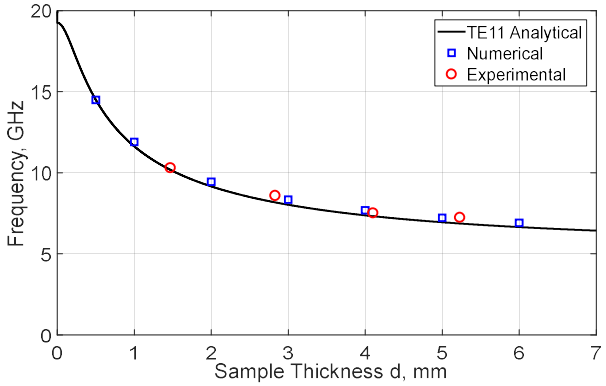

Fig. 6. Resonance frequency for TE_{11} mode as a function of sample thickness for the case of a dielectric sample with ε_r=13-j0.3.

A physical explanation of the resonance behavior is the following. Due to possible minor inhomogeneities in the sample, or a skew in the geometry of the sample surface, the fundamental *TEM* mode can transform into the higher-order modes, with the TE_{11} having the next lowest cut-off frequency and falling into the measurement band. The resonance for this mode can be excited along the sample length resulting in the

standing wave, and will exist until damped due to some loss in the sample.

Note that in perfect coaxial waveguides with axial symmetry, including axially aligned transitions from one cross-section to another, the axially symmetrical TEM mode in a coaxial structure cannot transform to asymmetrical TE modes [5]. This is because the electric field vector cannot suddenly change its direction in one side of the cross-section. However, if axial symmetry is violated so that the conditions for wave propagation are different in two halves of the cross-section of the coaxial waveguide, the asymmetrical TE modes can be excited and supported by the waveguiding structure [8]. This is the case of an imperfect (inhomogeneous, with a skewed face) sample in the coaxial line. The similar situation is observed, *e.g.*, when the center pins of the parts of the coaxial connector are imperfectly aligned [12].

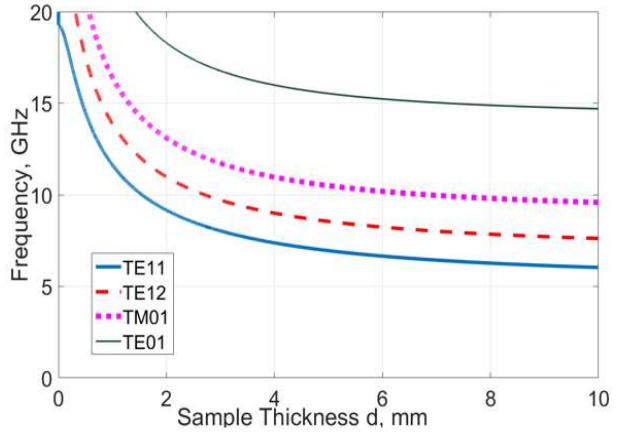

Fig. 7. Analytically modeled resonance frequency vs. dielectric (ε_r=13-*j*0.3) sample thickness for a number of higher modes in the coaxial 7/3-mm line

The analytically calculated curves of resonance frequency vs. sample thickness for a number of the other higher-order modes in the 7/3-mm coaxial line are shown in Fig. 7. The longer the sample thickness, the more important to account for the higher-order modes is, since resonances will take place at the lower frequencies and may be more intense.

V. Conclusion

This work demonstrates the importance of taking into account higher-order modes excited in the coaxial test fixture with a material sample under test. The theoretical foundation for description of higher-order mode behavior is presented. The results of numerical and analytical models unambiguously show that at least the lowest higher-order mode TE_{11} indeed can emerge. This mode may cause distortion of measured frequency dependences of the complex electromagnetic material parameters. Such possibility must be taken into account when preparing samples for tests. Excitation of higher-order modes results from possible inhomogeneities in a sample, especially at its interfaces with air in coaxial test fixtures. If axial symmetry due to an imperfect sample (or at the connector/adapter sides) is violated, the conversion from TEM mode to the higher-order modes may take place causing parasitic resonances. In thicker samples, the higher-order modes with corresponding parasitic resonances can emerge at lower frequencies.

To reduce the effect of the higher-order modes on measurements in a coaxial test fixture, samples should be as homogeneous as possible. Their interfaces with air should be as flat and smooth as possible to assure for strictly perpendicular to the TEM propagation vector in a coaxial waveguide. No gaps between the sample and the metallic surfaces of the test line are allowed. If a material under study has a high propagation constant, *i.e.*, high product of permittivity and permeability, the thickness of the sample should be such that the higher-order mode resonances are kept away from the frequency range of interest.

The proposed reason for higher-order parasitic resonances in TEM waveguiding structures with extended inhomogeneities, like composite samples under test, can be also applicable to the other practically important transmission line structures (with TEM or quasi-TEM propagation). The examples are the coaxial connector pins at the adaptors, or transitions from a coaxial pin to a microstrip or a stripline, including embedded filters on printed circuit boards. In any transmission line, if electromagnetic field structure changes due to inhomogeneity, an excitation of the higher-order modes and manifestation of the related resonance effects should be carefully examined, and the parasitic resonances should be avoided if possible.

Acknowledgment

The authors acknowledge financial support provided by the Russian Science Foundation, project no. 16-19-10490.

References

[1] L.F. Cheng, C.K. Ong, C.P. Neo, V.V. Varadan, and V.K. Varadan, *Microwave Electronics – Measurement and Materials Characterization*, Wiley, 2004.

[2] A.M. Nicolson and G.F. Ross, "Measurement of the intrinsic properties of materials by time-domain techniques," *IEEE Trans. Instr. Meas.*, vol. 19, pp. 377–382, Nov. 1970.

[3] W.R. Weir, "Automatic measurement of complex dielectric constant and permeability at microwave frequencies," *Proc. IEEE*, vol. 62, pp. 33–36. Jan. 1974.

[4] K. Rozanov, and M. Koledintseva, "Analytical representation for frequency dependences of microwave permeability", *IEEE Symp. Electromagn. Compat.*, Pittsburg, PA, 2012, pp. 422-427.

[5] E. Decrossas, M.A. El Sabbagh, V.H. Hanna, and S. M. El-Ghazaly, "Mode matching technique-based modeling of coaxial and circular waveguide discontinuities for material characterization purposes", *Int. J. Microw. Wireless Technologies*, vol. 3, no. 6, 2011, pp. 679-690.

[6] S. Lefrancois, D. Pasquet, and G. Maze-Merceur, "A new model for microwave characterization of composite materials in guided-wave medium", *IEEE Trans. Microw. Theory Tech.*, vol. 44, no. 9, pp. 1557-1562, Sept. 1996.

[7] FEKO Overview, https://altairhyperworks.com/product/FEKO, Altair – HyperWorks.

[8] J. Baker-Jarvis, M.D. Janezic, J.H. Grosvenor, Jr., and R. G. Geyer, "Transmission/reflection and short-circuit line methods for measuring permittivity and permeability", *NIST Tech. Note* 1355, Boulder, CO, USA, 1992.

[9] S. Ramo, J.R. Whinnery, and T. Van Duzer, *Fields and Waves in Communication Electronics*, Wiley, 3rd ed., 1994.

[10] C.A. Balanis, *Advanced Engineering Electromagnetics*, Wiley, 1989.

[11] D.M. Pozar, *Microwave Engineering*, Wiley, 2nd edition, 1998.

[12] M. Bailey, *Guidance on Selecting and Handling Coaxial RF Connectors Used with Rohde & Schwartz Test Equipment*, Application Note, 4.2015-1MA99_2e, Apr. 2015, http://www.rohde-schwarz.com/appnote/1MA99.